# Electronic Supplementary Information

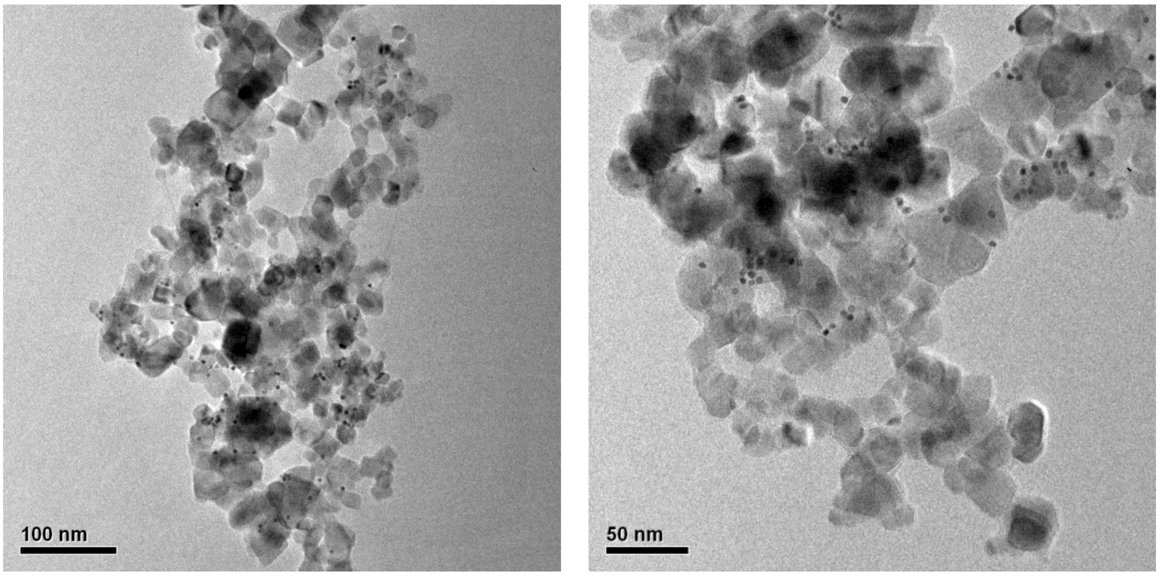

**Fig.S1** Pt/$TiO_2$ synthesized using colloidal deposition method

In the colloidal deposition method, Pt nanocrystals were pre-synthesized using $(NH_4)_2PtCl_4$ as metal precursor together with PVP and TMABr, similar to that of C. Tsung et. al [1]. $TiO_2$ (P25) was added to the solution containing Pt nanocrystals with vigorous stirring. Significantly agglomeration of Pt was found on $TiO_2$ surface [Fig.S1]. In order to get highly dispersion of Pt nanocrystals on $TiO_2$, the colloidal nanoparticles need to be synthesized at high dilute or be previously washed to remove the residue capping agent on Pt surface to get dispersed nanocrystal, which will decrease space time yields, increase costs, hamper its industrial application. Controlling the degree of removal capping agent is also a problem.

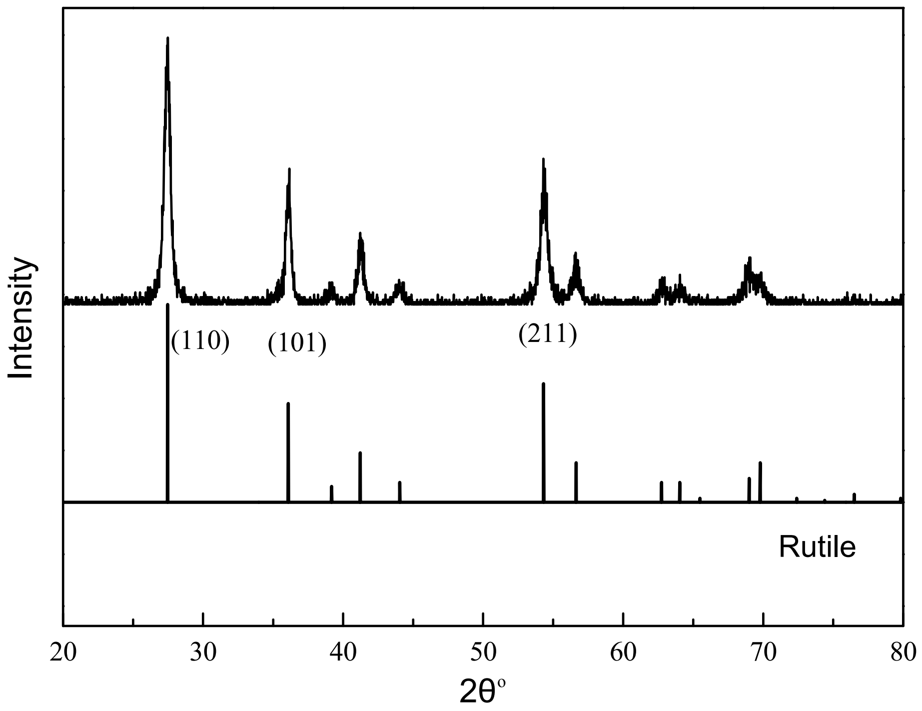

**Fig.S2** XRD pattern of rutile $TiO_2$

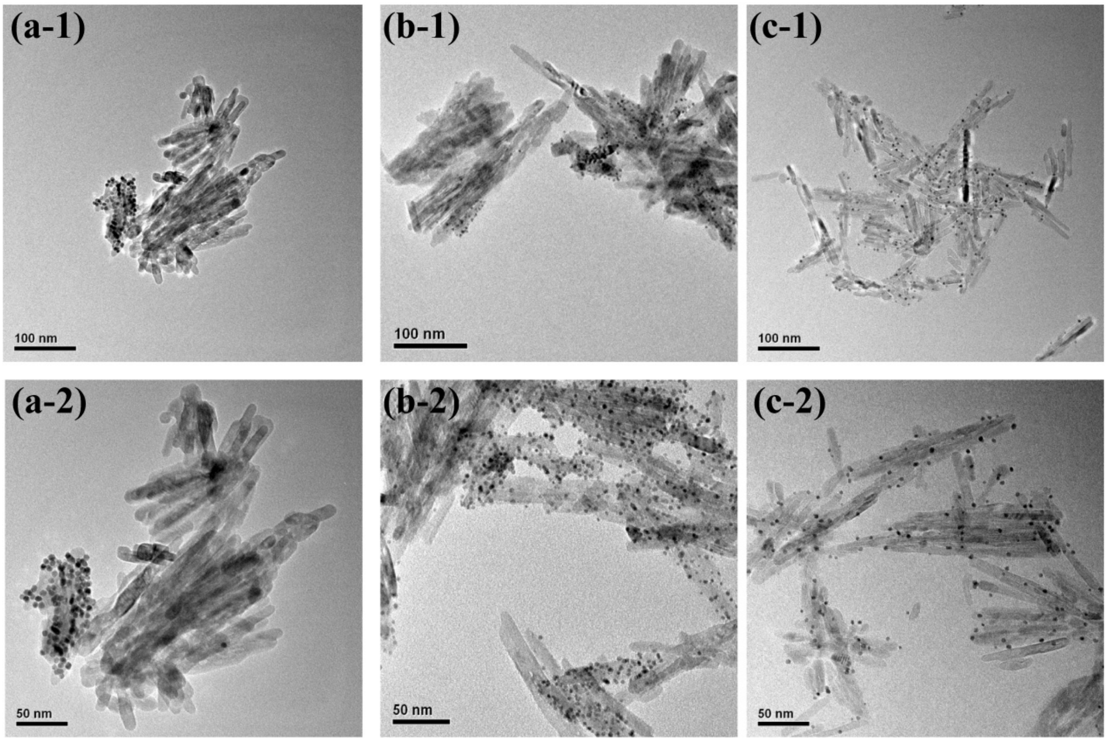

Fig.S3. Pt/$TiO_2$ synthesized without PVP (a-1,a-2), premixing $TiO_2$ and PVP at room temperature (b-1,b-2), premixing of PVP with $TiO_2$ in 60 °C and ultrasound for 30 minutes (c-1,c-2) using Pt (IV) salt ($H_2PtCl_6.6H_2O$) as metal salt precursor in ethylene glycol.

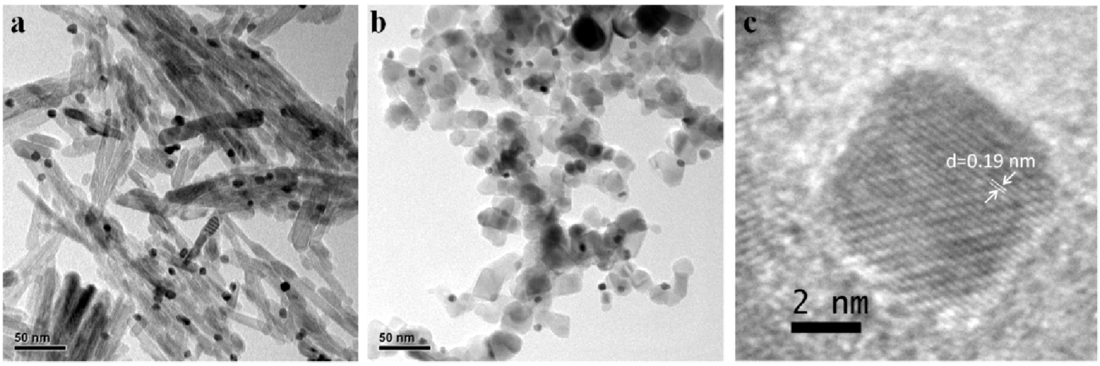

**Fig.S4** In-situ synthesis Pt nanocrystals on rutile $TiO_2$(a) P25 $TiO_2$ (b) respectively , using Pt (IV) ($H_2PtCl_6.6H_2O$) salt as metal salt precursor in ethylene glycol together with PVP and TMABr, high resolution image of cubic Pt supported on $TiO_2$(P25)(c)

Compared with in-situ synthesis Pt nanocrystals on $TiO_2$ surface using Pt(II) salt as precursor shown in Fig.1, using Pt (Ⅳ) salt in the same process produced well dispersed shaped cubic Pt nanocrystal on $TiO_2$ surface, the irregular shapes of byproducts consist of spheres and rectangular structures

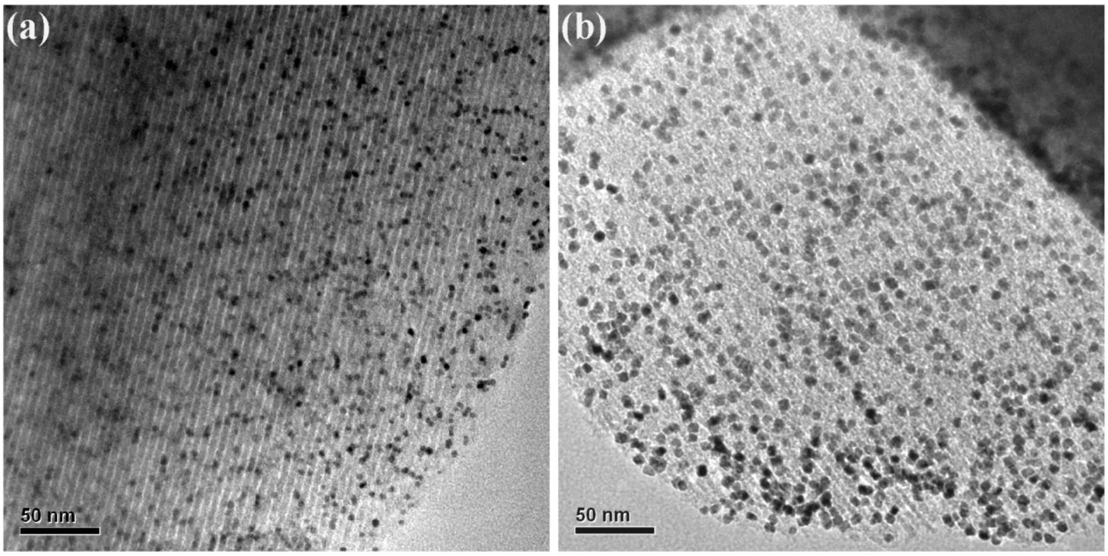

**Fig. S5** In situ synthesis Pt nanocrystals on $SiO_2$ (a homemade SBA-15), using Pt(II) salt ($(NH_4)_2PtCl_4$ ) (a) and Pt (□) salt ($H_2PtCl_6.6H_2O$) (b)as metal precursor respectively, together with PVP and TMABr

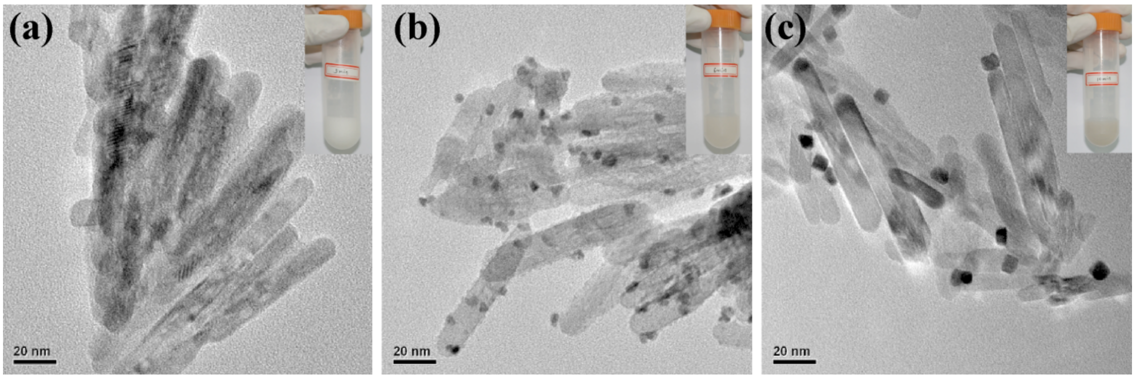

**Fig.S6** Pt/$TiO_2$ nanoparticles during the synthesis process: (a) 5 minutes (b) 6 minutes (c) 10 minutes

The growth of large shaped Pt particles on the $TiO_2$ surface (Fig.S4) provides opportunity to investigate the nature of the intermediate and whether the growth of the Pt is in-situ on the $TiO_2$ or not. When reduction of $H_2PtCl_6$ was carried out with $TiO_2$, PVP, TMABr in ethylene glycol under 180 $^oC$, the color of the solution changed in the following sequence: pale yellow, white, pale grey, and finally dark grey. Aliquots of the reaction solutions at 3, 5, 6, 10 minutes (typical 0.5ml) were extracted and rapidly cooled with acetone at 0 $^oC$ to quench the reaction. After centrifugation and washing with acetone, the samples were studied by using TEM. The treatments of rapid cooling and washings with acetone were to "freeze" the Pt/$TiO_2$ nanostructures so that they could be isolated and studied with TEM. The increase in particle size with reaction time during solution phase synthesis involves nucleation, growth, and other processes such as aggregation and coarsening. TEM results in Fig.S6 show that there is a slow and continuous nucleation process of Pt when Pt is reduced together with $TiO_2$ as no obvious Pt nanocrystals could be observed on $TiO_2$ surface and solution until 5 minutes reaction. The color of the mixture turned from white into pale grey after 6 minutes reaction. The initially formed irregularly shaped Pt nanoclusters of average size 4.08±0.7nm on the $TiO_2$ appeared in 6 minutes, suggesting the growth of Pt on $TiO_2$ becoming aggressively between 5 to 6 minutes. As the reaction progressed, the color of the reaction solution turn to darker, regular shaped Pt nanocrystals appears and the average size increases to about 6.1±0.6nm. TEM results provide evidence of slow continuous nucleation and fast in-situ surface growth mechanism of Pt in this one step in-situ process, suggesting that each Pt nucleus increases its size progressively on $TiO_2$ until the final nanocrystal particle is formed.

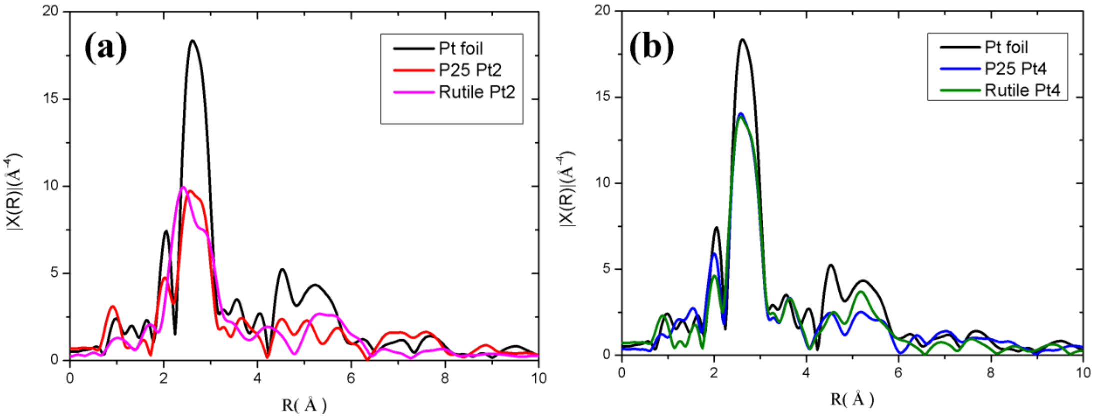

**Fig.S7** X-ray absorption studies: radial distribution functions of synthesized Pt/$TiO_2$: using $(NH_4)_2PtCl_4$ as metal precursor, samples shown in Fig.1 (a); using $H_2PtCl_6.6H_2O$ as metal precursor, samples shown in Fig.S4 (b)

## DFT calculation

The formation of well-dispersed Pt nanocrystals with controlled size and shape is partly due to the competition between the adsorption of Pt atom on $TiO_2$ surface and formation of Pt cluster. To understand this competition, we investigated the adsorption of $Pt_n$ ($n$=1, 2, 4, and 18) clusters on rutile $TiO_2$ (110) surface based on the first-principles calculation. The first-principles calculations are performed within the framework of spin-polarized plane-wave density functional theory (DFT), implemented in the Vienna ab initio simulation package (VASP) [2,3], within the generalized gradient approximation with the Perdew-Burke-Ernzerhof (PBE) functional[4] and projector-augmented-wave potentials (PAW). The dipole correction was considered [5,6]. The $TiO_2$ (110) surface was modeled with a four-layer slab in which the two bottom layers are kept at their bulk positions. A supercell containing 3×2 surface unit cells is used when studying the adsorption of Pt and $Pt_2$ on $TiO_2$ surface. Upon $Pt_4$ and $Pt_{18}$ clusters, a big supercell containing 6×2 surface unit cells is used. The nearest distance between two neighboring Pt cluster is larger than 8 Å. The vacuum region is set as 12 Å. An energy cutoff of 400 eV is used for the plane wave expansion of the electronic wave function. The first Brillouin zone is sampled with 2×2×1 Monkhorst-Pack k-point grids. Geometry structures were relaxed until the force on each atom was less than 0.01 eV/Å, and the convergence criteria for energy is $10^{-4}$ eV, respectively.

## UV/$O_2$ Pre-treatment

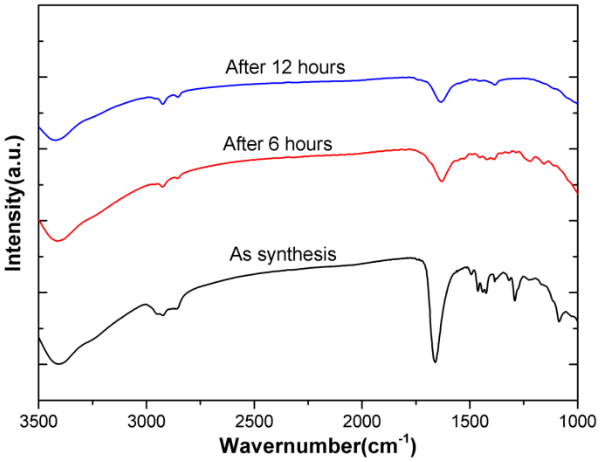

**Fig.S8** FT-IR spectra of Pt/$TiO_2$ under UV treatment at 0, 6, 12 hours under the irradiation of full-arc light

The UV/$O_2$ photocatalysis oxidation cleaning effect was followed by IR spectroscopy. The Pt/$TiO_2$ (in-situ polyol process) is the Pt/P25 shown in Fig.1c. The details of PVP IR bands can be found elsewhere [7]. The evolution of the IR spectra for the Pt/$TiO_2$ under UV/$O_2$ for 6 hours and 12 hours in the range of the C-H stretching (2700-3200 cm$^{-1}$) and fingerprint region (1250-2000 cm$^{-1}$) was shown in Fig.S8. The intensity of band decreased a lot during the first 6 hours and the fingerprint region for PVP vibration (1250-2000 cm$^{-1}$) completely disappeared after 12 hours photocatalysis oxidation. The decrease in the IR signal results from the elimination of PVP. The IR-spectra suggested that the photocatalysis oxidation is a simple and green way to remove the remaining surfactant on the surface of $TiO_2$. Pt/$TiO_2$ (rutile) showed similar surfactants elimination behavior under the same pretreatment condition. It is also noteworthy that although the in-situ polyol process could be extrapolated to other oxides, such $SiO_2$[Fig.S5], the followed light-induced photocatalysis oxidation process just could be applied on photocatalysts with the capability to decompose PVP[8].

## Photocatalytic Activity for hydrogen Production

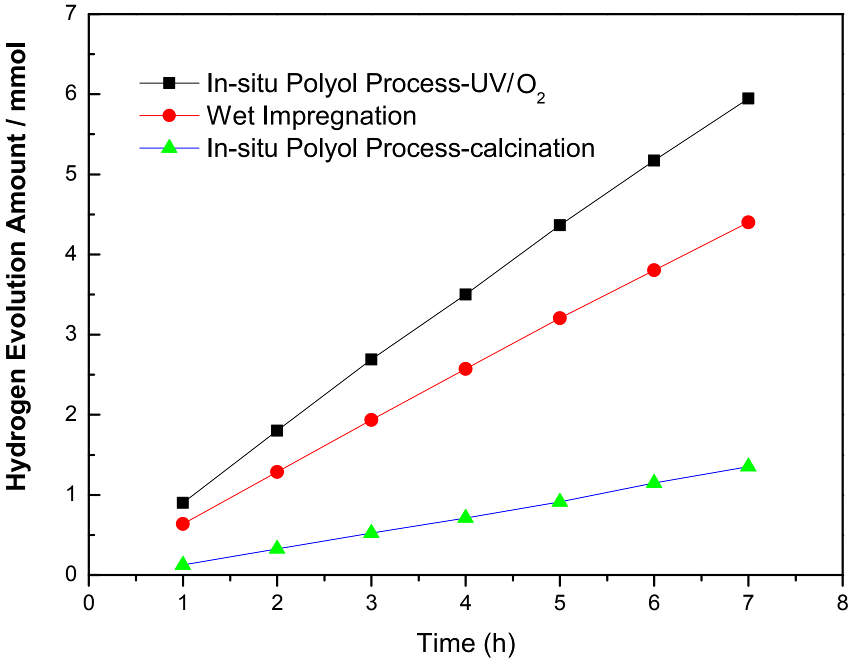

**Fig.S9** Photocatalysis hydrogen production amount from water/methanol for Pt/$TiO_2$ prepared by in-situ polyol process/UV-$O_2$ process, in-situ calcination process and wet impregnation respectively. In the calcination process, the catalysts were heated to 350 $^{o}$C in air at heating rate of 2 °C/min and keeping at that temperature for 4 hours.

The photocatalytic activities for hydrogen evolution from water using methanol as holes sacrifice are summarized in Fig.S9. As shown in Fig.S9, the $H_2$ evolution amount for the three samples was stable since the first 1 hour and during the 7 hours test time. $H_2$ evolution amount for the Pt/P25 (in-situ polyol/UV-$O_2$) was 35% higher than that of Pt/P25 (wet impregnation), which may indicate the effective separation of photo generated hole-electron pairs facilitated by the high dispersion of Pt nanocrystals on P25 surface prepared by in-situ polyol process. $H_2$ evolution amount for the Pt/P25 (in-situ polyol/UV-$O_2$) was 225% higher than that of Pt/P25 (in-situ polyol/calcination process). The significant decrease of photocatalysis activity for Pt/P25 (in-situ polyol/calcination process) compared with Pt/P25 (in-situ polyol/UV-$O_2$) may due to the active sites blocking resulting from calcination.

## Experimental

### Chemicals:

Chloroplatinic acid hexahydrate (IV) ($H_2PtCl_6.6H_2O$, 99%; Sinoreagent), Ammonium tetrachloroplatinate(II)($(NH_4)_2PtCl_4$,99%;Sigma-Aldrich),Titaniumtetrachloride($TiCl_4$>99.9%;Sinoreagent),$TiO_2$(P25;Deguass),poly(vinylpyrrolidone)(PVP,Mw=29000;Sigma-Aldrich),tetramethylammonium bromide (TMABr, 98%; Sinoreagent), Ethylene glycol(>99%; Sinoreagent) and solvents (analytical grade) including acetone, ethanol, and hexanes were used without further purification.

### $TiO_2$ Synthesis:

In a typical preparation of rutile $TiO_2$, 60 ml $TiCl_4$ solutions (0.6 M) was charged into a 100 mL Teflon-lined stainless steel autoclave in a heated furnace maintained at 130 $^oC$ for 12 hours. After the autoclave apparatus was cooled to room temperature in 2 hours, the product (suspension) was allowed to stand for 24 hours and was filtered after removing the supernatant, washed with water and alcohol several times till PH to 7, and dried at 80 $^oC$ and calcined at 300 $^oC$ for 2 hours.

### Pt/ $TiO_2$ Catalysts Prepared by in-situ polyol process

The platinum precursor and heating rate is controlled to yield platinum nanocrystals with tailored shape and size [1]. In a typical synthesis, 115 mg of tetramethylammonium bromide(TMABr), 111mg of PVP and calculated amounts of $TiO_2$ powders(2 wt% Pt) were dissolved into 10 mL of ethylene glycol in a 100 mL round-bottom flask at 60 $^oC$ and ultrasound for 30 minutes. A total of 0.05 mmol of Pt ions $H_2Pt(IV)Cl_6.6H_2O$ or $(NH_4)_2Pt(II)Cl_4$, was added to the mixture and the mixed solution was heated quickly to 180 °C in oil bath. The solutions were held at this temperature for 25 minutes under argon protection and magnetic stirring, resulting in a dark brown solution. After the solution was cooled to room temperature, the solution was centrifugation at 3000 rpm for 5 minutes. The dark blue product was collected by discarding the colorless supernatant. The products were further washed three times by precipitation/dissolution (re-dispersed in 10 mL of ethanol and then precipitated by adding 40 mL of hexanes).

### Pt/ $TiO_2$ Catalysts Prepared by wet impregnation method

For wet impregnation method, Pt/ $TiO_2$ catalysts were prepared by impregnating weighted $TiO_2$ supports with calculated amounts of $(NH_4)_2Pt(II)Cl_4$ aqueous solution, followed by 30minutes ultrasonic dispersion. Then the catalyst were dried at 110°C for 12 hours followed by calcined in air and $H_2$ at 400 °C for 4 hours respectively.

### Characterization Methods

Shape, size of the nanocrystals was analyzed using TEM (JEOL 2100HT and FEI Tecnai G2 F20 S-TIWN). X-ray diffraction patterns were measured on a Rigaku D/Max-2200/PC X-ray diffractometer. IR spectra were measured on a FTIR spectrometer (A Nicolet 6700 from Thermo Nicolet Corp., Madison, WI). Pt L3-edge absorption spectra (XAFS) were performed on the BL14W1 beamline at the Shanghai Synchrotron Radiation Facility (SSRF), Shanghai Institute of Applied Physics (SINAP), China, operated at 3.5 GeV with injection currents of 140–210 mA. Si(111) double-crystal monochromator was used. The harmonic rejection mirror was used to reduce high order harmonic component of the monochrome beam. Pt foil were used as reference samples and measured in the transmission mode, and all samples were measured in mode by Lytle detector. We used IFEFFIT software to calibrate the energy scale, to correct the background signal and to normalize the intensity on analyze the EXAFS data at the Pt L3 edge.

**Photocatalysis Oxidation After-treatment**

Top-irradiation Pyrex reaction cell with 28.26 cm$^2$ effective irradiation area is used in photocatalytic oxidation. The reaction cell is connected to an oxygen bubbling system with oxygen flow rate at 100 ml/min. In all experiments, the 0.2 g photocatalyst powder was suspended in 80 ml water solution. The temperature for all the photocatalytic reactions was maintained at 25 ± 5 °C. A 300-W Xenon lamp was used as the light source. The dark blue product after irradiation was collected by discarding the colorless supernatant after centrifugation. The products were further washed three times by precipitation/dissolution (re-dispersed in water 40 mL) and dried in vacuum oven in 353K for 12 hours before FT-IR and photocatalysis experiment.

**Photocatalysis Hydrogen Production Measurement:**

Top-irradiation Pyrex reaction cell with 28.26 cm$^2$ effective irradiation area is used in photocatalytic hydrogen evolution. The reaction cell is connected to a vacuum system for vacuuming before hydrogen evolution. After hydrogen evolution performance under lamp, the evolved hydrogen was analyzed by a thermal conductivity detector (TCD) gas chromatograph (China; GC-9200, MS-5A zeolite column, argon as the carrier gas). In all experiments, the 0.2 g photocatalyst powder was suspended in water-methanol solution (water 45 mL, methanol 20 mL), in which methanol played a role as the sacrificial agent to scavenge photo-generated holes. The temperature for all the photocatalytic reactions was maintained at 25 ± 5 °C. A 300-W Xenon lamp was used as the light source. P25 $TiO_2$ used in in-situ polyol process was pretreated in air and $H_2$ for 4 hours respectively to make sure the in-situ polyol $TiO_2$ is similar with the wet impregnation method.

**Reference**

1. Tsung, C.; Kuhn, J. N.; Huang, W.; Aliaga, C.; Hung, L., Somorjai, G. A.; Yang, P. J. Am. Chem. Soc., 2009, 131,5816-5822
2. Kresse, G. ; Furthmuller.J. Phys. Rev. B 1996, 54, 11169—11186
3. Kresse, G.; Furthmuller, J. J. Comput. Mater. Sci. 1996, 6, 15-50.
4. Perdew, J. P.; Burke, K.; Ernzerhof, M. Phys. Rev. Lett. 1996, 77, 3865-3868.
5. Blochl, P. E. Phys. Rev. B. 1993, 47, 558-561.
6. Kress, G.; Joubert, D. Phys. Rev. B. 1996, 59, 1758-1775.
7. Borodko, Y.; Habas, S. E.; Koebel, M.; Yang, P.; Frei, H.; Somorjai, G. A. J. Phys. Chem. B 2006, 110, 23052-23059
8. Horikoshi,A.; Hidaka, Hisao; Serpone, Nick; J. Photochem Photobio A: Chem 2001, 138: 69–77